

CO2 enclathration in the presence of water-soluble hydrate promoters: Hydrate phase equilibria and kinetic studies in quiescent conditions

Jean-Philippe Torre, Marvin Ricaurte, Christophe Dicharry, Daniel Broseta

▶ **To cite this version:**

Jean-Philippe Torre, Marvin Ricaurte, Christophe Dicharry, Daniel Broseta. CO2 enclathration in the presence of water-soluble hydrate promoters: Hydrate phase equilibria and kinetic studies in quiescent conditions. Chemical Engineering Science, 2012, 82, pp.1-13. 10.1016/j.ces.2012.07.025 . hal-02002062

HAL Id: hal-02002062
https://hal.science/hal-02002062

Submitted on 31 Jan 2019

HAL is a multi-disciplinary open access archive for the deposit and dissemination of scientific research documents, whether they are published or not. The documents may come from teaching and research institutions in France or abroad, or from public or private research centers.

L'archive ouverte pluridisciplinaire **HAL**, est destinée au dépôt et à la diffusion de documents scientifiques de niveau recherche, publiés ou non, émanant des établissements d'enseignement et de recherche français ou étrangers, des laboratoires publics ou privés.

OATAO
Open Archive Toulouse Archive Ouverte

Open Archive Toulouse Archive Ouverte

OATAO is an open access repository that collects the work of Toulouse researchers and makes it freely available over the web where possible

This is an author's version published in: http://oatao.univ-toulouse.fr/21853

Official URL: https://doi.org/10.1016/j.ces.2012.07.025

To cite this version:

Torré, Jean-Philippe and Ricaurte, Marvin and Dicharry, Christophe and Broseta, Daniel *CO2 enclathration in the presence of water-soluble hydrate promoters: Hydrate phase equilibria and kinetic studies in quiescent conditions.* (2012) Chemical Engineering Science, 82. 1-13. ISSN 0009-250

Any correspondence concerning this service should be sent to the repository administrator: tech-oatao@listes-diff.inp-toulouse.fr

CO_2 enclathration in the presence of water-soluble hydrate promoters: Hydrate phase equilibria and kinetic studies in quiescent conditions

Jean-Philippe Torré *, Marvin Ricaurte, Christophe Dicharry, Daniel Broseta

Univ. Pau & Pays Adour, CNRS, TOTAL – UMR 5150 – LFC-R – Laboratoire des Fluides Complexes et leurs Réservoirs, BP 1155 – PAU, F-64013, France

- ► Search of efficient additives for CO_2 capture processes using clathrates hydrates.
- ► Experimental results based on phase equilibria, kinetics and visual observations.
- ► Action mechanisms linked to these additives are analysed and discussed.
- ► Mixed CO_2+THF hydrate promote the formation of the single CO_2 hydrate.
- ► Potentialities of this combination of additives (SDS+THF) are demonstrated.

Keywords:
Gas Hydrates
Carbon dioxide
Phase equilibria
Kinetics
Separations
Additives

A B S T R A C T

Clathrate hydrates have potential applications in various domains and particularly for CO_2 capture where the search for additives able to speed up hydrate formation is of scientific, technological and economical interest. This study investigates the potentialities of two additives used in combination for enhancing CO_2 enclathration rates: a surfactant (sodium dodecyl sulphate; SDS) and an organic compound (tetrahydrofuran; THF). Experiments performed in batch and in semi continuous reactor configuration, reveal that this combination of additives efficiently promotes hydrate formation, allowing a full water to hydrate conversion despite the quiescent forming conditions used. The possible action mechanisms of this combination of additives are analyzed and discussed on the basis of experimental data of hydrate phase equilibria (with and without additives), visual observations, and kinetics experiments.

1. Introduction

Clathrate hydrates (usually called simply *hydrates*) represent active areas of research from a fundamental level to a practical one (Sum et al., 2009). These stuctures are solid non stoechiometric inclusion compounds formed by a lattice structure, composed of water molecules (named *host* molecules) linked together by hydrogen bonding, and stabilized by encapsulating a variety of small molecules (named *guest* molecules). Numerous compounds have been reported to form clathrate hydrates, including gas species (e.g., H_2, CH_4, CO_2), as well as low molecular weight organic compounds, e.g. acetone, cyclopentane (CP) and tetrahydrofuran (THF). The type of crystal structure formed depends on the chemical nature, the size and shape of the guest molecule. The two most common structures are referred to "structure one" denoted (sI) and "structure two" denoted (sII). The (sI) structure, which observed, e.g. with CO_2 or CH_4, contains 8 cavities: two small pentagonal dodecahedral cavities denoted 5^{12} and 6 large tetra(kai)decahedral cavities denoted $5^{12}6^2$, with 46 water molecules per unit cell. The (sII) structure, observed with larger molecules, e.g. THF or CP, contains 16 small 5^{12} cavities and 8 large $5^{12}6^4$ hexa(kai)decahedral cavities, with 136 water molecules per unit cell (Sloan, 2003).

While hydrate research continues to be of paramount importance in relation to flow assurance in the oil and gas industry, novel applications of hydrates are investigated in various domains such as gas transportation and storage, refrigeration and air conditio ning applications, exploitation of potential sources of natural gas from permafrost and marine sediments (combined or not with CO_2 sequestration), water treatment (desalination), and gas separa tion processes (Sun et al., 2011). Among the various innovative solutions proposed to capture CO_2, hydrate based processes may be more effective and more advantageous than conventional CO_2 sepa ration methods (such as cryogenic fractionation, chemical/physical absorption, adsorption processes or membranes), which exhibit

* Corresponding author. Tel.: +33 0 5 40 17 51 09; fax: +33 0 5 79 40 77 25.
E-mail address: jean-philippe.torre@univ-pau.fr (J.-P. Torré).

http://dx.doi.org/10.1016/j.ces.2012.07.025

(in some cases) high energy costs, insufficient capacity, corrosion problems or large amounts of chemicals used (Figueroa et al., 2008; Sun et al., 2011). Gas separation techniques based on the use of clathrate hydrates appears as a promising alternative and an economical option (Duc et al., 2007), which could be particularly interesting in applications where the inlet gas containing CO_2 is available at high pressure and the separated CO_2 is to be reinjected in a geological formation. Thus, the technique being at the "proof of concept" stage today is considered to be an interesting option on the long term (Kuramochi et al., 2011).

Various studies have already discussed the effective separation by gas hydrate formation of various mixed gases containing carbon dioxide (Eslamimanesh et al., 2012). In recent years, different efficient processes have been tested, including stirred vessels, spray or jets reactors, bubble columns, and mesoporous media (Kang and Lee, 2010; Sun et al., 2011). However, one major bottleneck associated to hydrate based CO_2 capture processes remains the slow hydrate formation kinetics.

In comparison to hydrate phase equilibria studies, kinetic data of hydrate formation and dissociation, particularly for CO_2 hydrates, are rather scarce (Sabil et al., 2010). One manner to enhance the hydrate formation kinetics is to add *suitable* additives to water. With the same operating conditions, one possibility is to displace to higher temperatures and lower pressures the equilibrium conditions where hydrate forms by using a class of additives named *thermodynamic promoters*. Tetrahydrofuran (THF), which is a cyclic aliphatic ether, is one of the most investigated guest thermodynamic promoter, used in many hydrates studies as a reference system, because THF is able to form with water a (sII) stoechiometric hydrate (THF $17H_2O$) at atmospheric pressure and moderately low temperature (Makino et al., 2005). In presence of CO_2 or CH_4, a small amount of THF is able to very significantly reduce the pressure and increase the temperature of formation of a mixed hydrate which contains both the gas to be captured (CO_2 or CH_4) and THF (Sabil et al., 2009; Seo et al., 2003). For instance, when only 3.8 wt% of THF added to water, the formation pressure of a mixed CO_2+THF hydrate at 280 K is about one fifth of the formation pressure necessary to form the single CO_2 hydrate (Delahaye et al., 2006).

Other additives, referred to as *kinetic promoters*, enhance the hydrate formation kinetics without modifying the thermodynamic equilibrium of the systems studied. For instance, sodium dodecyl sulfate (SDS), a widely used anionic surfactant, is well known to have excellent kinetic promoting effects with respect to hydrocarbon hydrate formation (Yoslim et al., 2010), at very low dosage (Gayet et al., 2005), and without using any mechanical stirring (Okutani et al., 2008). However, the same surfactant (used without any other additive) seems to be rather ineffective in promoting CO_2 hydrate formation (Zhang and Lee, 2009). Although the ability of various compounds for enhancing hydrate formation kinetics has been mentioned for more than a decade (Zhong and Rogers, 2000), the mechanisms by which these promoters increase the hydrate formation rate are not fully understood and hardly debated (Di Profio et al., 2005; Rogers et al., 2007; Zhang et al. 2010).

In addition, the possibility to enclathrate the CO_2 in the absence of any mechanical agitation (that is in quiescent conditions) by means of suitable additives would minimize risks of gas leakages through the agitator gland packing, static electricity and sparks problems, particularly when the reactor is maintained under pressure during reaction and when the gas used is potentially hazardous and flammable (Watanabe et al., 2005). As argued recently by Linga et al. (2010), the energy requirement necessary to maintain sufficient mechanical stirring of the hydrate slurry prevent the development of large scale and cost competitive CO_2 capture processes. In fact, achieving high water to hydrate conversion and acceptable kinetics under quiescent conditions (i.e., in the absence of agitation) is really a challenge.

Surprisingly, although THF and SDS are very commonly used for various purposes in hydrate research or applications, the effects of these two molecules used in combination are poorly documented (Liu et al., 2008a, 2008b *written in Chinese*; Zhu et al., 2011). The main conclusions drawn from these studies are: (i) the use of these two additives in combination drastically reduces the induction time (defined as the time elapsed until the appearance of a certain detectable quantity of hydrate phase); (ii) the kinetics of CO_2 enclathration depends on the concentration of the additives. However, further work is still necessary to understand the action of these two molecules. In the present paper, we investigate the influence of this combination of additives on the CO_2 enclathration rate in quiescent conditions, both in batch and in semi continuous reactor configurations.

This paper first presents experimental CO_2 hydrate equilibrium curves obtained with and without the SDS and/or THF as additives. Then, kinetic data of CO_2 enclathration in quiescent hydrate forming conditions are presented in the presence or absence of SDS and/or THF. The first part of the kinetic experiments was conducted in *batch reactor configuration*, where the influence the additives was investigated, and where the batch tests were used to define the optimum operating conditions ("optimal reactor pressure") for the ensuing *semi continuous* isobaric experiments. These latter experiments are detailed in the second part of the paper, where the effect of the THF concentration was investigated at constant driving force during hydrate formation. Then, the effect of this combination of additives on the CO_2 enclathration kinetics and the possible action mechanisms are analyzed and discussed.

2. Experimental apparatuses and materials

2.1. Experimental rigs

2.1.1. Experimental rig used for phase equilibria studies

The hydrate formation and dissociation curves presented in Section 3 were carried out using the experimental apparatus (denoted *Rig #1*) shown in Fig. 1.

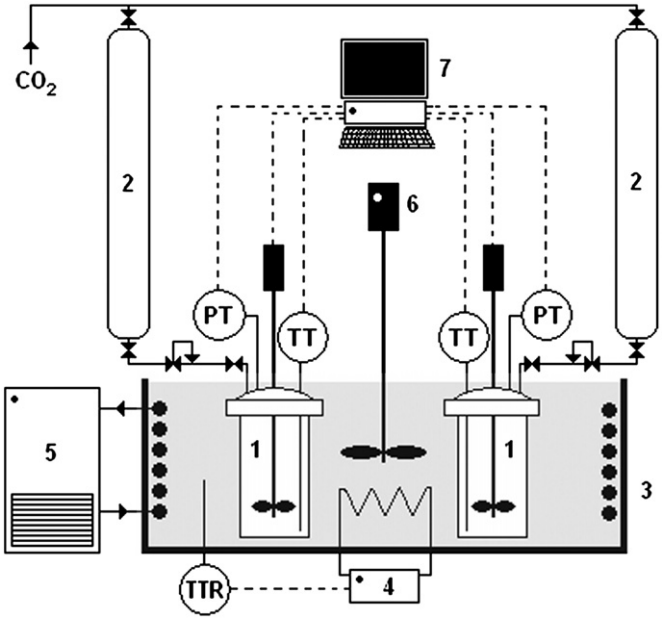


Fig. 1. *Rig* #1 used for thermodynamic studies: (1) hydrate forming agitated reactor; (2) gas storage vessel; (3) insulated bath; (4) heater; (5) cryostat; (6) bath agitator; (7) data acquisition system (standard PC).

The rig is equipped with two identical 316L stainless steel high pressure cells (hydrate forming stirred reactors from Parr Instru ments Company) entirely immersed in a fully insulated tempera ture controlled bath. Each cell is connected to its own CO_2 storage vessel which allows, through a pressure reducing valve, the gas to be charged into the cell at the desired pressure. The diameter of each cell is 33 mm, and the total cell volume is 128 ± 0.5 cm^3 (including the reactor top dome and fittings). For all experiments reported in Section 3, the rotation speed of the agitator was maintained constant at 800 rpm. The reactors and bath tempera tures are measured using PT100 probes and the pressure inside the cells with 0 25 MPa transducers. All the data are monitored and recorded in continuous using a standard PC equipped with Specview© supervision software. The experimental accuracies for the determination of hydrate equilibrium data (taking account of technical specifications, data acquisition and repeatability tests) with Rig#1 are estimated to be ± 0.2 K for temperature and ± 0.03 MPa for pressure measurements.

2.1.2. Experimental rigs used for kinetic studies

As underlined by Koh et al. (2011), the measurements of hydrate formation kinetics are generally plagued with reproduci bility problems, and are often equipment dependent data. There fore, for the kinetic studies reported in this paper, two different rigs denoted *Rig #2a* and *Rig #2b* were used. The main part of the kinetic data presented in this paper was obtained with *Rig #2a*, with additional experiments performed on *Rig #2b* to examine the robustness of the main data set.

The two rigs were built according to the same design shown in Fig. 2.

Each rig allows running experiments up to pressures of 20 MPa in the range of temperature from 263 to 323 K. The hydrate forming reactor is a jacketed high pressure cell made in 316 L stainless steel except for the inner shell which is in titanium TA6. The internal volume of the reactor is of 168.0 ± 0.9 cm^3 for *Rig #2a*, and of 174.0 ± 0.9 cm^3 for *Rig #2b*. Each reactor is equipped by a star shaped magnetic agitator of 20 mm diameter driven by a magnetic stirrer located on the bottom of the cell. Two sapphire windows of 20 mm diameter and placed at 180° from each other are mounted on the cell. They allow lighting inside the reactor and observing the different hydrate morphologies inside the reactor with a camera (LiveCam Optia AF from Creative Labs). The liquid and gas temperatures are measured with a precision of ± 0.2 K by two PT100 probes, and the reactor pressure is mea sured with a 0 10 MPa pressure transducer with an accuracy of ± 0.02 MPa. The CO_2 storage vessel used to feed the reactor is a cylindrical 316 L stainless steel vessel of internal volume of 382.2 ± 0.5 cm^3, where the gas temperature and pressure are measured by using a PT100 probe with an accuracy of ± 0.2 K, and a 0 20 MPa pressure transducer with a precision of ± 0.03 MPa. A pressure reducing valve coupled to a digital manometer allows adjusting the pressure of the feed gas in the cell to the desired value. The monitoring and data acquisition are done using a standard computer (PC) equipped with a LabView™ interface in which the acquisition frequency has been set to 1 Hz for all experiments. The precision given of all of the sensors have been estimated, integrating the data acquisition system and the repeatability of the measurements.

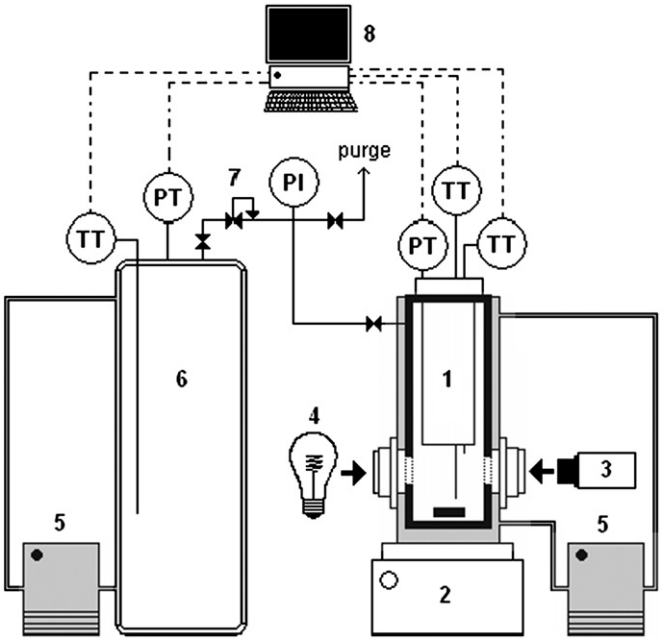


Fig. 2. *Rigs #2a and Rig #2b* used for kinetic studies: (1) hydrate forming reactor; (2) magnetic stirrer; (3) camera; (4) lighting system; (5) thermostatic baths; (6) CO_2 storage vessel; (7) pressure-reducing valve and (8) data acquisition system (standard PC).

The reactor can be operated in two different configurations: *batch* and *semi continuous*. In the *batch configuration*, the reactor is isolated from the CO_2 storage vessel and hydrate formation takes place under isochoric conditions. In the *semi continuous* (or *semi batch*, *or isobaric*) *configuration*, fresh gas is delivered continuously to the reactor under constant pressure and hydrate formation takes place under isobaric conditions. It is important to note that, although the agitation system of the reactor is efficient for enhancing gas solubilization, it is not capable of maintaining any hydrate slurry in suspension: the agitator is immediately stopped as soon the crystallization begins and hydrates grow in quiescent conditions. The reactor is thus qualified as a *quiescent hydrate forming reactor*.

2.2. Materials

The gas used in this work is carbon dioxide (CO_2) provided by Linde gas (purity 99.995%). Chemicals used are sodium dodecyl sulfate (SDS) from Chem Lab (purity > 98%) and tetrahydrofuran (THF) from Sigma Aldrich (purity > 99.9%). All aqueous solutions are prepared using ultra pure water (resistivity of 18.2 MΩ cm) produced in our laboratory by a PureLab Classic from ELGA Labwater. The solutions containing the additives THF+SDS are always prepared by first dissolving the desired amount of SDS into 50 ml of ultra pure water, then adding the desired mass of THF, and finally adjusting under agitation the total mass of the solution with ultra pure water to 200.00 ± 0.01 g.

3. Hydrate phase equilibria of $CO_2/H_2O/SDS$ and $CO_2/H_2O/THF/SDS$ systems

Prior to the kinetic studies, the influence of the two additives (THF and SDS) on hydrate phase equilibria is assessed from formation/dissociation experiments, which consist in monitoring the reactor temperature (T^R) and reactor pressure (P^R) during a hydrate formation/dissociation cycle. In a cycle, the hydrate phase is first formed from the aqueous solution and gas by cooling the system deep enough into the hydrate stability zone (HSZ), and then the hydrate(s) formed are slowly dissociated by heating at a low rate. This cycle is hysteretic in character, i.e. temperature and pressure differ in the formation and dissociation stages, due to metastability. A strong departure from equilibrium conditions (or 'driving force') is usually required for hydrate formation, whereas the dissociation part of the hysteresis curve follows

(for a pure component) the three phase (hydrate, aqueous solu tion and gas) equilibrium conditions if the heating rate used for hydrate decomposition is slow enough. The objectives of these experiments are (i) to confirm that the presence of 0.3 wt% SDS in water has no influence on the dissociation curves of the pure CO_2 hydrates and the mixed CO_2+THF hydrates, and (ii) to obtain experimental data of the CO_2+THF mixed hydrate dissociation curves for the specific concentrations of THF used later in the kinetic studies (1 wt% and 4 wt%).

3.1. Experimental protocol

The experimental apparatus used in this section is *Rig* #1 shown previously in Fig. 1. The two reactors of this rig are run simultaneously under exactly the same temperature conditions. A volume of 50.00 ± 0.05 cm^3 of the aqueous solution containing the additive(s) is introduced first in each reactor. The reactor is sealed, connected to the rest of the equipment, immersed into the bath regulated at the temperature of 293.0 ± 0.2 K, and purged two times with CO_2. CO_2 is then loaded in the reactor under strong stirring of the aqueous phase in order to accelerate CO_2 dissolution until the target pressure is reached: this corresponds to point A in Fig. 3.

The reactor is then closed and its P T conditions are driven deep into the HSZ (path AB in Fig. 3) by decreasing the tempera ture down to a value not smaller than 274 K (the temperature target could be different from one experiment to the other). Hydrate formation starts at point B in Fig. 3 and manifests itself both by a small increase of T^R and by a rapid decrease in reactor pressure (path BC). Finally, the reactor pressure stabilises when the three phase equilibrium pressure for that temperature is reached (at point C). Then, T^R is raised back to its initial value by applying a heating rate of 2.5×10^{-3} K/min: the system follows the hydrate dissociation path CD corresponding to the three phase equilibrium curve for the system investigated in Fig. 3 (the CO_2/water+SDS system). The last crystal of CO_2 hydrate is dissociated at point D, as denoted by the breaking point on the dissociation curve. In the last portion of the curve (from D to E), the system returns to its initial pressure and temperature conditions. In all experiments, the pressure variation between the initial and final points (points A and E, respectively) turns out to be inferior to 0.05 MPa (which is acceptable for the experiments carried out here). The minor difference between the two hysteresis curves shown in Fig. 3 (corresponding to two different experiments) demonstrates the very good reproducibil ity of the method, and therefore, only one curve will be presented in the following figures for the sake of clarity.

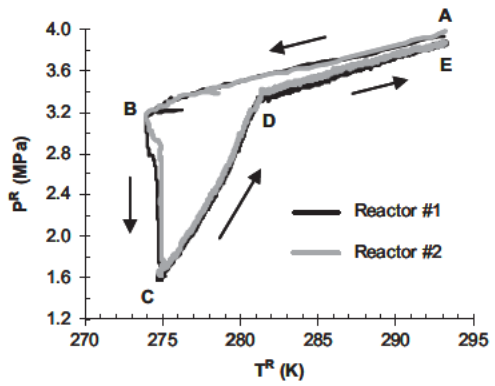


Fig. 3. Hydrate formation/dissociation hysteresis curves obtained with the system H_2O+SDS using the two reactors of the *Rig* #1. SDS concentration is 0.3 wt%.

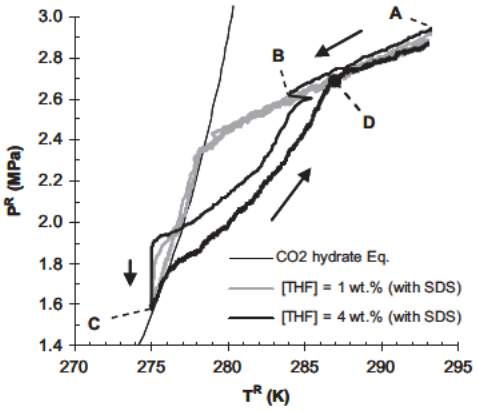


Fig. 4. Hysteresis curves obtained with two different initial THF concentrations in the aqueous phase (grey bold line: [THF] 1 wt%; black bold line: [THF] 4 wt%). SDS concentration is 0.3 wt% in the two experiments. The solid regular line is the CO_2 hydrate equilibrium curve obtained with CSMGem (Sloan and Koh, 2008).

3.2. Results and discussion

Fig. 4 presents the hydrate formation/dissociation hysteresis curves obtained experimentally from 293 to 275 K with different initial THF concentrations in the aqueous phase (1 wt% and 4 wt%) and a SDS concentration of 0.3 wt%. Several studies (Sum et al. 1997, Shin et al. 2009) have already proved that, when CO_2, water and THF are present under suitable thermodynamic conditions, a mixed CO_2+THF hydrate of structure (sII) is formed, where the large and small cavities are partially occupied by THF and CO_2, respectively.

With an initial THF concentration in the aqueous phase of 4 wt%, the first exothermic peak observed (Fig. 4, point B) at T^R=284.0 K together with an immediate pressure decrease, shows very clearly that the expected mixed CO_2+THF hydrate forms firstly. Then, as the system enters the pure CO_2 hydrate stability zone, the reactor pressure (P^R) continues to drop until the pure CO_2 hydrate equilibrium curve is reached (point C in Fig. 4). During the dissociation, the pure CO_2 hydrate dissociates firstly (the hysteresis curve first follows the CO_2 hydrate equilibrium curve). Then, the mixed CO_2+THF hydrates dissociates progres sively. Contrary to the situation in the absence of THF, the equilibrium curve of the mixed CO_2+THF hydrate cannot be obtained with a single dissociation experiment as THF and water form a liquid binary mixture. Therefore, several experiments are required as only the point where the last crystal of mixed hydrate dissociates: this corresponds to a "breaking point" on the dis sociation curve (represented by the point D in Fig. 4). As shown in Fig. 4, in the case where 4 wt% of THF is used, the successive events of hydrate formation and dissociation occur for tempera tures and pressures that differ strongly from each other, and can therefore be unambiguously distinguished. However, as shown in Fig. 4, when the THF concentration in water is equal to 1 wt%, the equilibrium curves of the mixed CO_2+THF hydrate and of the pure CO_2 hydrate can hardly be distinguished from each other.

The hydrate equilibrium points obtained experimentally are plotted in Fig. 5, where our data are compared to other data found in the literature. The pure CO_2 hydrate equilibrium curve has also been determined using the same experimental protocol from 278.0 K to 282.3 K.

Our data on CO_2 hydrate equilibrium agrees with the experi mental data of Vlahakis et al. (1972) and with the values obtained using the CSMGem model (Sloan and Koh, 2008), confirming the robustness of our experimental protocol. The comparison between the equilibrium data obtained with and without adding SDS in water demonstrates clearly that the addition of 0.3 wt% of

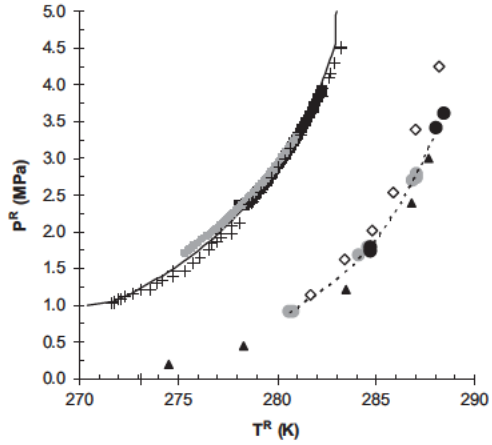


Fig. 5. Comparison of our data with other data sets: hydrate equilibrium data for CO_2 hydrate and mixed CO_2+THF ([THF] 4 wt%) obtained with and without adding 0.3 wt% of SDS. (+) CO_2 hydrate equilibrium data from Vlahakis et al. (1972); (■) our equilibrium data of CO_2 hydrate; (■) our equilibrium data of CO_2 hydrate with SDS; (◇) CO_2+THF hydrate equilibrium data from Shin et al. (2009); (●) our equilibrium data of CO_2+THF hydrate; (●) our equilibrium data of CO_2+THF hydrate with SDS; (▲) CO_2+THF hydrate equilibrium data from Delahaye et al. (2006); the regular solid line is CO_2 hydrate equilibrium from CSMGem (Sloan and Koh, 2008); the dashed line is a polynomial fitted curve of the THF+CO_2 mixed hydrate equilibrium data (our data with and without SDS) as a visual guide.

SDS in water has no influence (on a thermodynamic point of view) on CO_2 hydrate equilibrium. The equilibrium data obtained with 4 wt% of THF (with and without SDS) are reported in Table 1.

It is clearly apparent in Fig. 5 that the addition of 4 wt% THF in water allows hydrates to form in the presence of CO_2 at a distinctly higher temperature and lower pressure, confirming the important promoting thermodynamic effect of THF. A good agreement is observed between our data and those from Delahaye et al. (2006) obtained with [THF]=3.8 wt% and those from Shin et al. (2009) obtained with [THF]=3.9 wt%. In addition, no shift in the mixed hydrate equilibrium curve is observed when 0.3 wt% of SDS is added to the (water+THF) phase (similarly to CO_2 hydrate equilibrium).

4. Kinetic experimental studies

4.1. Experiments in batch reactor configuration

4.1.1. Experimental protocol and type curves

The experimental apparatus used in this section is *Rig #2a* presented previously in Fig. 2. Concerning the experimental protocol, a volume of 65.0 ± 0.1 cm^3 from a freshly prepared aqueous solution is first charged into the reactor (the water/gas denoted *w/g* interface is located in the middle of the reactor see through windows). The reactor is then closed, connected to the rest of the experimental rig, and brought under agitation to the temperature of 293 K (agitation speed: N=600 rpm). When temperature is stabilized, the agitation is stopped and the reactor is vented three times with CO_2. Then CO_2 is loaded again into the reactor to reach the desired pressure and a time period of around one minute is left for temperature equilibration. The magnetic stirrer is then started again at N=600 rpm to speed up CO_2 solubilization into the aqueous solution. The pressure into the CO_2 storage vessel decreases with time and stabilizes to a constant value when equilibrium is reached. The reactor is maintained under agitation in isobaric (P^R=2.70 MPa) and iso thermal conditions (T^R=293 K) during at least two hours to allow for complete CO_2 solubilization.

Table 1
Experimental equilibrium data of CO_2+THF mixed hydrate (with and without SDS). [THF] 4 wt% and [SDS] 0.3 wt%.

T^R (K)	P^R (MPa)
With SDS	
280.8	0.91
280.6	0.91
284.6	1.79
284.1	1.68
287.0	2.78
287.0	2.74
286.9	2.70
Without SDS	
284.7	1.73
284.7	1.79
288.4	3.60
288.0	3.41

In batch configuration, the reactor is isolated from the CO_2 storage vessel. The temperature of the cryostat is decreased with a cooling ramp of 0.9 K/min to a target value of 275 K (this temperature is held constant till the end of the experiment). Fig. 6(a) shows a typical evolution of the reactor pressure and temperature as a function of time, together with snapshots of the *w/g* interface in an experiment carried out with an aqueous solution containing initially 4 wt% THF and 0.3 wt% SDS, an initial loading pressure of 2.70 MPa, and quiescent hydrate forming conditions (the case where [THF]=1 wt% will be commented later in Section 4). The temperature and pressure conditions of the various snapshots (labelled by letters A, B, C, etc.) are indicated both in Fig. 6(a) and (b) showing the corresponding *P T* diagram where the following hydrate equilibrium data curves have been superimposed: the pure CO_2 hydrate equilibrium data from CSMGem (Sloan and Koh, 2008) and our experimental equilibrium data (obtained with 4 wt% of THF) for the mixed CO_2+THF hydrate (see Section 3).

Snapshot A in Fig. 6(a) shows the aspect of the solution during the solubilization stage: the liquid is transparent, and a vortex deforms the liquid free surface due to vigorous stirring. The agitation of the aqueous phase is maintained in the reactor during the reactor cooling period in order to speed up CO_2 solubilization and keep the system as close as possible to equilibrium. The appearance of the aqueous phase is carefully monitored, and stirring is turned off as soon as the aqueous phase becomes turbid: this occurs at point B in Fig. 6(a). It is observed (snapshot B) that an important quantity of solids is produced quasi instan taneously over the whole bulk. This first crystallization is accom panied by a noticeable exothermicity (the temperature in the liquid rises suddenly by several degrees) as shown in Fig. 6(a) and (b) (point C), whereas the reactor pressure continues to decrease. It can therefore be interpreted as being due to a gas hydrate crystallization process, which is hereafter referred to as "*first hydrate*" formation. Then, a solid like layer grows up onto the reactor windows as shown in snapshots D to F, while the reactor pressure continues to decrease.

Following point E, the reactor pressure begins to decrease at a much higher rate showing that the rate of hydrate formation increases strongly. Interestingly, it can be seen very distinctly that, from points F to H, the hydrate(s) formed previously on the reactor window dissociates progressively while CO_2 is being captured at a high rate. The pressure decrease rate goes through a maximum represented by the black dot (determined numeri cally) in Fig. 6(a), and which coincides with a second smaller exothermicity peak observed on the temperature vs. time curve (point G). The end of the CO_2 enclathration process (point H)

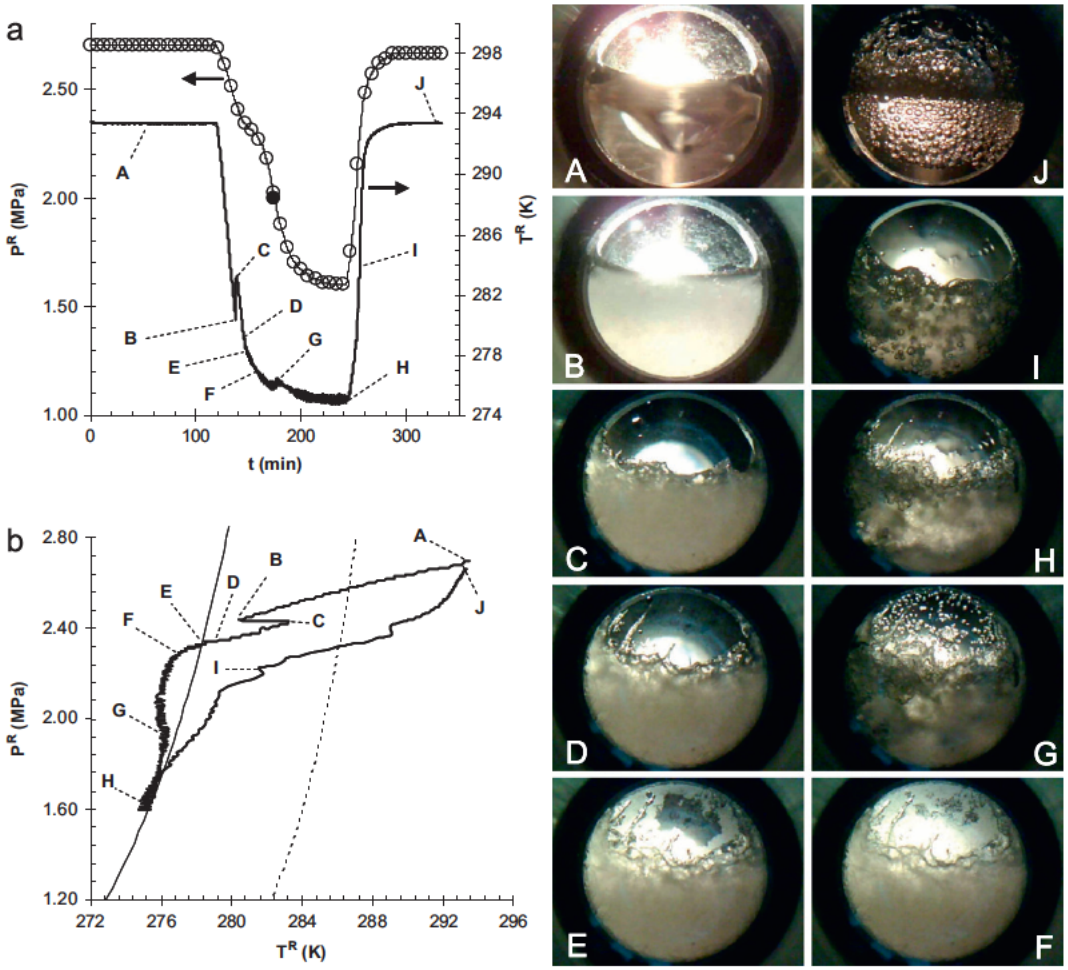


Fig. 6. Type curves corresponding to a CO_2 enclathration experiment carried out in batch configuration, initial reactor pressure 2.70 MPa, [THF] 4 wt%, [SDS] 0.3 wt%. (a): reactor pressure and temperature as a function of time ; (b) *P–T* diagram corresponding to the experimental data, the regular line is the CO_2 hydrate equilibrium from CSMGem (Sloan and Koh, 2008), the dashed line is the CO_2+THF mixed hydrate equilibrium curve (our data) obtained with [THF] 4 wt%.

corresponds to the stabilization of the reactor pressure at a constant value equal to the pure CO_2 hydrate equilibrium pres sure for the reactor temperature of 275 K (see Fig. 6(b)). When the hydrate formation is finished, the temperature of the cryostat is raised back to 293 K in order to dissociate all the hydrates formed (see snapshot I for example). The reactor pressure reaches progressively a value very close to the initial pressure level (difference inferior to 2%) and the liquid level returns to its initial value as shown on the final snapshot J.

4.1.2. *Influence of the presence of additives*

A series of experiments has been conducted to study the influence of the presence of THF and/or SDS on the CO_2 encla thration kinetics in quiescent hydrate forming conditions. Fig. 7 presents the reactor temperature and pressure as a function of time in four distinct and characteristic situations: (i) no additive is present (pure water), (ii) only THF at a concentration of 4 wt% in water, (iii) only SDS at a concentration of 0.3 wt% in water, and (iv) SDS and THF are present in concentrations equals to 0.3 wt% and 4 wt%, respectively. The experimental protocol is the same as that described in the previous subsection. For simplification purposes, the reactor pressures and temperatures are represented in Fig. 7 starting from the end of the gas solubilization period, and ending about 600 min after the end of the solubilization period (but some experiments last much longer).

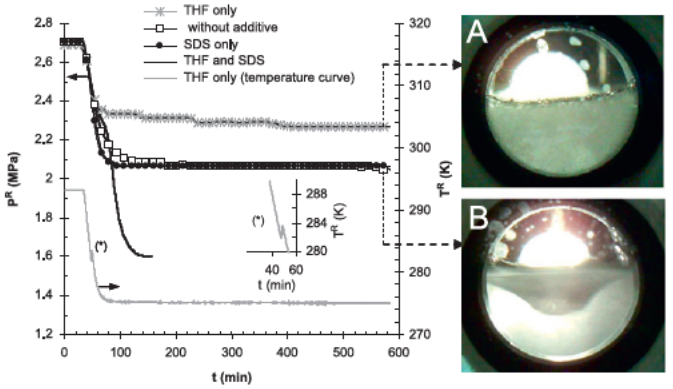


Fig. 7. Comparison of four different kinetic curves (reactor pressure and temperature versus time) obtained with and without additives. [THF] 4 wt%, [SDS] 0.3 wt%.

The evolution of the reactor temperature and pressure and the visual aspect of the *w/g* interfaces are extremely different, depending on whether or not THF and/or SDS are present in the water phase:

(i) When water is pure, hydrates do not form upon cooling the reactor down to 275 K and maintaining it at this temperature more than 540 min (nine hours) under agitation.

(ii) When only SDS is present in water, the observations and conclusions are identical to those in the absence of SDS (case (i)): hydrates do not form. In addition, the presence of 0.3 wt% SDS in water has no noticeable effect of the quantity of CO_2 dissolved in the solution, as evidenced by the identical final pressure, even though CO_2 dissolves in the aqueous phase more rapidly than in the absence of SDS (Ricaurte et al., 2012). In some experiments where the reactor is maintained under agitation at T^R=275 K during more than two days, hydrate crystallisation is not observed. As shown in snapshot B of Fig. 7, the initially transparent solution ends up in a turbid liquid, indicating that the reactor temperature is below the Krafft temperature where SDS is no longer soluble in water.

(iii) When only THF is present in water, the formation of the "first hydrate" occurs (at T^R=281.8 K and P^R=2.47 MPa). This hydrate formation is easily identified by the small exothermic peak visible (inset presented in Fig. 7) in the temperature curve. After this first crystallisation, the reactor pressure decreases very slowly and no "high rate" CO_2 enclathration takes place. This observation has been confirmed by several experiments. In addition, the morphology of the solid observed at the end of the experiment is shown in snapshot A. The bulk liquid contains a large quantity of white solid, in appearance compact, and no crystallisation on the reactor window is observed in this case.

(iv) When THF and SDS are present, a very different behaviour is observed. As discussed in previous subsection, pressure dramatically decreases shortly after the formation of the "first hydrate", and eventually reaches the equilibrium pressure of the pure CO_2 hydrate at the temperature considered (275 K here). The influence of the additives concentrations on the kinetic curves has been described previously in Torré et al. (2011a): in short, the enclathration rate depends on SDS concentration and a SDS concentration superior or equal to 0.15 wt% is suitable to enclathrate CO_2 at high rate in a reasonable time (that is the reason why a concentration of 0.3 wt% is used here); this rate also depends on THF concentrations and a minimum of 1 wt% of THF in solution is suitable (that is why the concentrations of THF investigated here are 1 and 4 wt%).

4.1.3. Discussion

As discussed previously, when THF and CO_2 are present together, a mixed CO_2+THF with hydrate structure (sII) forms first when temperature is lowered, with large cavities occupied by THF and small cavities by CO_2. In Fig. 6(b), it is obvious from the position of the exothermicity peak located between the two hydrate equilibrium curves (of pure CO_2 and mixed CO_2+THF hydrates) that the crystallization observed at this point is that of the mixed hydrate CO_2+THF. However, the determination of the exact composition of this mixed hydrate and the filling occupancy of the cages would require for example the use of spectroscopic techniques, such as Raman or NMR (Rovetto et al., 2007; Seo et al., 2003), which was not available in our laboratory. Assuming that all THF is enclathrated in this "first hydrate" (a mixed CO_2+THF hydrate), the solid which then appears and grows (particularly upon the see through window, see Fig. 6) is attributed to pure CO_2 hydrate formation. This "second hydrate" formation occurs in fact close to the equilibrium conditions of the pure CO_2 hydrate, meaning that the "first hydrate" which is present in the bulk acts as a powerful "catalyst" (or precursor) of the ensuing second formation of pure CO_2 hydrates. The same mechanism has been already suggested by Zhang and Lee (2009) for CO_2 hydrate formation in presence of cyclopentane (CP is also a very good "thermodynamic promoter" of (sII) hydrates), and Uchida et al. (2004) who suggested that the existence of hydrate crystals in the system help to nucleate other hydrate crystals. Finally, the reactor pressure drastically decreases due to hydrate formation and CO_2 enclathration stops because the reactor pressure reaches the pure CO_2 hydrate equilibrium pressure. This observation, already mentioned by others (Liu et al., 2008a; Torré et al., 2011a), is one of the most robust evidence that the hydrate which forms from the mixed CO_2+THF hydrate is pure CO_2 hydrate.

Concerning the experiments carried out in presence of SDS, it is worth noting that the concentration used here (0.3 wt%) is slightly higher than the critical micelle concentration (CMC) at ambient conditions (CMC_{SDS}=0.23 wt% at 298 K according to Rana et al. (2002)). However, SDS solubility has been found to be only a function of temperature and to not vary significantly in presence of CO_2 and with the gas pressure (Zhang et al. 2007). Few authors (Bakshi, 1993; Lopez Grio et al., 1998) have shown that the addition of small amounts of water soluble organic additives (such as THF, acetonitrile, methanol, or DMSO) may influence micelle formation, interfacial properties and CMC. In addition, various Krafft temperatures of SDS in water at ambient pressure conditions (i.e., in the absence of any dissolved gas in water) have been reviewed by Watanabe et al. (2005), who proposed an averaged value at T_K(SDS)=285 ± 4 K. However, to the best of our knowledge, nothing was found in the open literature concerning the influence of THF on the Krafft points of SDS aqueous solutions. Thus, SDS precipitation at the temperature of interest here (T^R=275 K) is very likely (as shown in snapshot B of Fig. 7), but interfacial properties and Krafft points of SDS in the presence of both THF and CO_2 in aqueous solution need to be further investigated.

One of the possible explanations why CO_2 enclathration is very efficient when THF and SDS are used jointly (even in quiescent conditions) may be that the action of the two additives confers a porous structure to the hydrates formed into the bulk, which then remains continuously permeable to CO_2. Note that the formation a hydrate layer or crust at the *w*/*g* interface preventing gas/liquid transfer has never been observed in the presence of both additives, which supports the proposed scenario. Concerning the possible mechanisms responsible for this behaviour, Zhang et al. (2008, 2010) have suggested (on the basis of zeta potential measurements) that the dissociated DS anions adsorb on THF hydrate and thus keep this hydrate in dispersed form due to electrostatic repulsion between hydrate particles. The adsorption of SDS has also been claimed by Lo et al. (2010) to occur onto cyclopentane hydrates on the basis of Raman spectroscopy: these authors argued that the adsorption at the water hydrate interface causes hydrogen bond water molecules to arrange in the same manner that they are in hydrates, and proposed that this mechanism could enhance the intrinsic enclathration rate.

The formation of a "porous" hydrate structure in the bulk could also be explained by the coexistence of different hydrates and/or structures (Schicks and Ripmeester (2004)). In our case, there are at minimum two different coexisting hydrates: the mixed CO_2+THF hydrate of structure (sII) which forms firstly, and the CO_2 hydrate which forms later. Another assumption is that the presence of the "first hydrates" of structure (sII) in the bulk acting as a template, it could be possible that a metastable form of CO_2 hydrate of structure (sII) was formed transiently. Metastable (sII) hydrates formed with guests usually known to form (sI) hydrates have been already observed and characterized by Staykova et al. (2003) with CO_2 as the guest molecule, and by Schicks et al. (2006) with methane. Schicks and Ripmeester (2004) have also argued that, when a (sII) precursor is already present, a metastable phase of methane hydrate (sII) can form and is the kinetically favored structure compared to the methane hydrate (sI). This observation

has also been reported by Moudrakovski et al. (2001) with Xenon (the smallest hydrate former known to form (sI) hydrate), which can form s(II) metastable Xe hydrate when a powdered (sII) THF hydrate is initially present. In our experiments, the growth of a hydrate film on the reactor see through window as soon as the CO_2 hydrate equilibrium curve is crossed, and then the rapid decom position of this solid (phenomenon visible in the snapshots of Fig. 6) might be linked to this formation of (sII) metastable CO_2 hydrate. This film may grow first by contact with the (sII) CO_2+THF mixed hydrate present initially in the bulk, and then, as this structure is not thermodynamically stable, decompose into a more stable (sI) structure. Unfortunately, this assumption cannot be verified for the moment as it needs adapted in situ Raman, NMR or XRD measurements.

4.2. Experiments in semi continuous reactor configuration

4.2.1. Experimental protocol and types curves

When the system is operated in a semi continuous configura tion, fresh gas is continuously fed in the reactor under constant pressure while gas hydrates are forming. The constant pressure chosen for the experiments in the semi continuous configuration reported below is that corresponding to the maximum CO_2 enclathration rate determined in the previous set of batch experiments (see Section 4.1), to which the system is brought according to the same procedure as that described in Section 4.1. This "optimum" pressure turns out to be fairly reproducible and independent of parameters such as THF concentration (from 1 to 4 wt%) and initial pressure (from 2.43 to 3.50 MPa): its mean value as estimated from a total of 33 batch experiments is equal to 1.89 MPa with a standard deviation of 0.08 MPa (see Appendix A). The semi continuous experiments reported below have been carried out with a THF concentration in the aqueous solution of either 1 wt% or 4 wt%, an initial pressure equal to 2.7 MPa and a SDS concentration equal to 0.3 wt%. The purposes of these experiments are: (i) to demonstrate the feasibility of a quiescent semi continuous process to capture CO_2 by hydrate crystalliza tion by using the SDS+THF combination of additives; and (ii) to investigate whether the quantity of THF has any influence on the CO_2 enclathration rate and on the total amount of CO_2 captured in the hydrate phase. Most experiments are performed with *Rig #2a*, whereas a few experiments are carried out with *Rig #2b* to check for the reproducibility and robustness of the results.

The experiments thus entail two distinct and consecutive periods:

1. In the *initial period*, the reactor is used as described in previous subsection: CO_2 is first solubilized in the aqueous phase, and the system is then cooled down into the region of hydrate formation while pressure decreases down to the pressure of maximum CO_2 enclathration rate (1.89 MPa),
2. when this "optimum" pressure is reached, the *semi continuous period* starts, i.e., the reactor is switched from batch to semi continuous configuration by opening up a manual valve which allows feeding the reactor with fresh gas at the desired constant pressure (P^R=1.89 MPa).

The results of a typical experiment, carried out with 1 wt% of THF and 0.3 wt% of SDS, are depicted in Fig. 8(a), which shows the evolution of the reactor and CO_2 storage vessel pressures versus time, and the reactor temperature versus time. Fig. 8(b) presents the corresponding path in the *P T* diagram (same experiment) where the Lw H V equilibrium curves of pure CO_2 and mixed CO_2+THF hydrate are also represented. Snapshots of the *w/g* interface at various times (labelled A, B, C, etc.) are also shown in Fig. 8.

The solubilization period and the initial aspect of the solution (snapshot A) are indeed identical to those observed when the reactor is operated in batch configuration (see previous section). Note that, in parallel to the reactor cooling, the temperature of the CO_2 storage vessel is decreased from 293 to 283 K in order to pre cool the gas which will be later brought to the reactor (this temperature of 283 K was chosen to prevent the CO_2 liquefaction into the CO_2 storage vessel). At this THF concentration (1 wt%), the crystals of the *first hydrate* formed in the bulk of the aqueous phase (see snapshot B of Fig. 8) are observed to settle down rapidly and form a solid like deposit visible in the bottom of the reactor window (snapshot C) for a temperature slightly above the target temperature of 275 K (the agitator is switched off as soon as the solution becomes turbid). As discussed in previous subsec tion, the formation of this "*first hydrate*" is accompanied by a noticeable exothermicity: the temperature of the liquid phase rises suddenly (see the inset in Fig. 8(a)), whereas the reactor pressure continues to decrease; a solid like layer grows up very quickly on the reactor windows (snapshot D), while solid particles continue to be formed in the bulk (snapshot E).

When the reactor is switched to the semi continuous config uration, the pressure of the CO_2 storage vessel decreases with elapsed time due to the CO_2 consumption needed for hydrate formation, as shown in Fig. 8(a). Snapshots F, G and H of Fig. 8 show evidence of rapid water consumption: the level of liquid in the reactor decreases rapidly and drops down to below the bottom of the see through windows. This observation agrees with the mechanism referred to "capillary driven" in which hydrates grows on the cold reactor shell (we have verified this by opening our reactor at the end of the CO_2 enclathration), and this porous structure pumps the aqueous phase by capillarity (Gayet et al., 2005; Zhang and Lee, 2009). Finally, the reactor temperature decreases slowly from about 276 K to the target temperature of 275 K, whereas the pressure of the CO_2 storage vessel stabilizes to a constant value, signifying that hydrate formation has ended.

4.2.2. Results and discussion

On the basis of the results of the thermodynamic studies (Section 3) and of the batch experiments (Section 4.1), we have concluded previously that the *first hydrate* generated in the bulk (seen in snapshot B of Fig. 8) is attributed to the mixed CO_2+THF hydrate. Therefore, one of the most interesting features is that, similarly to the situation (detailed in Section 4.1) in which the aqueous phase is more concentrated (4 wt%) in THF, the rapid generation of a few crystallites of mixed CO_2+THF hydrate in the bulk of the aqueous phase (with 1 wt% THF) is sufficient to immediately promote the formation of pure CO_2 hydrate.

The CO_2 molar quantity entering the reactor in the semi continuous period (i.e. leaving the CO_2 storage vessel), denoted $\Delta n^{SV}_{CO_2}$, is presented in Fig. 9 as a function of the time elapsed since the beginning of the semi continuous period for the two THF concentrations investigated (1 and 4 wt%). This quantity is inferred from the (isothermal) pressure variation in the CO_2 storage vessel using the Peng Robinson equation of state (PR EoS). The results from seven independent experiments car ried out with *Rig #2a* for each of the two THF concentrations investigated are reported in Fig. 9, from which reliable values of two quantities of interest namely the CO_2 enclathration rate in the semi continuous period (dn_{CO_2}/dt) and the total CO_2 consumption over the semi continuous period ($\Delta n^{SV}_{CO_2}\big|_{tot}$) can be calculated. The experimental data exhibit some scatter, which thus can be quantified from the repeated experiments.

It can be remarked that, for the two THF concentrations tested, this rate is fairly constant over a large period of time. This behaviour

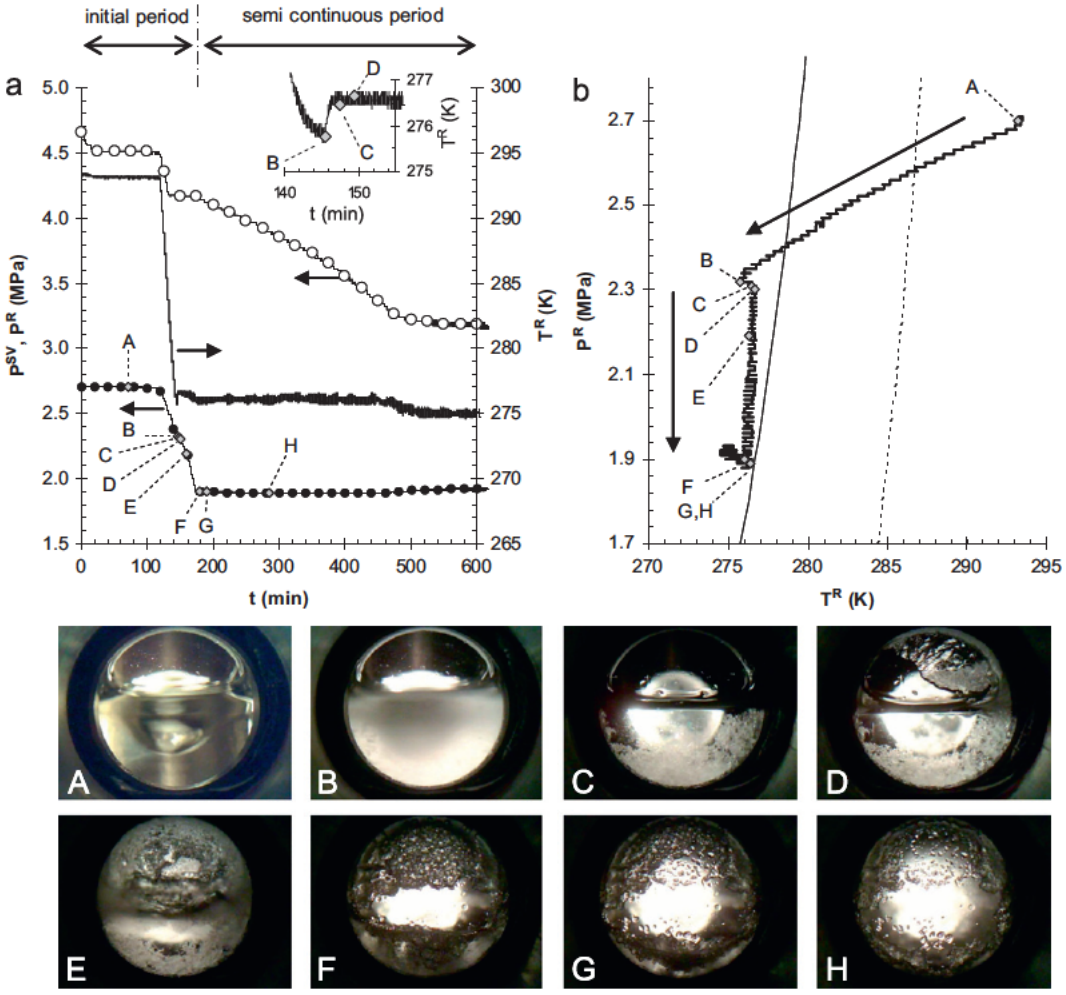


Fig. 8. Type curves for a typical experiment carried out in semi-continuous configuration with [THF] 1 wt%, [SDS] 0.3 wt%, initial reactor pressure 2.70 MPa and P^R 18.9 MPa in the semi-continuous period. (a) Evolution of the reactor pressure P^R, reactor temperature TR and gas storage vessel pressure P^{SV} versus time; (b) Evolution of the reactor pressure versus rector temperature (bold line); full regular line is the CO_2 hydrate equilibrium from CSMGem (Sloan and Koh, 2008); dashed line is our equilibrium data for the mixed CO_2+THF hydrate with 4 wt% THF. Snapshots are extracted from the video recorded during the experiment.

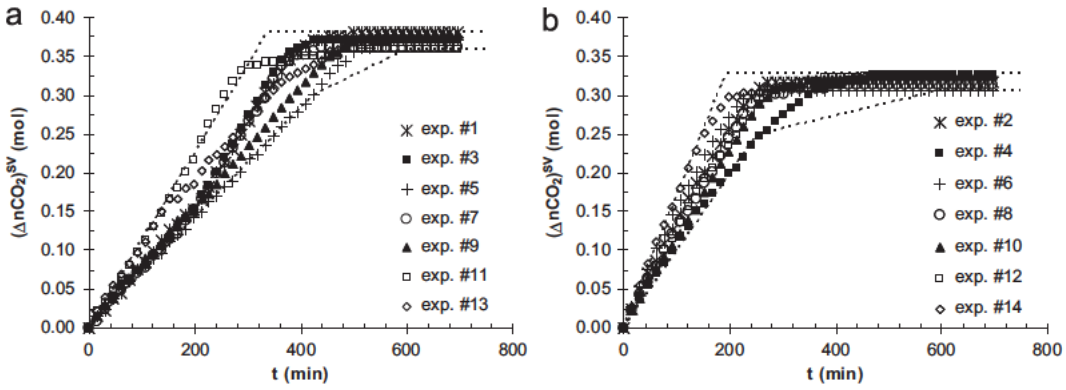


Fig. 9. CO_2 consumption in the storage vessel versus time elapsed since the beginning of the semi-continuous period. (a) [THF] 1 wt%; (b) [THF] 4 wt%. [SDS] 0.3 wt%. Dashed lines represent the min–max envelope of the data.

is consistent with a pseudo first order kinetics, such as that of the well known *Englezos Kalogerakis Dholabhai Bishnoi* model (Ribeiro and Lage, 2008). In the data range where this first order behaviour holds (i.e., for $\Delta n^{SV}_{CO_2} < 0.3$ mol for [THF]=1 wt%, and for $\Delta n^{SV}_{CO_2} < 0.25$ mol for [THF]=4 wt%), linear fits of the two data sets provide the values of the *average* CO_2 enclathration rates $(dn_{CO_2}/dt)_{avg}$, which are reported in Table 2 together with the total CO_2 consumption during the semi continuous period.

In addition, one experiment has been carried out for each THF concentration (1 and 4 wt%) on the other rig (*Rig #2b*) using the same protocol: the results are shown in Fig. 10 together with the maximum and minimum enclathration rates observed in the

Table 2
Numerical values of the CO_2 enclathration rates and total CO_2 consumptions in the semi-continuous period (min, average and max values) on the two rigs (*Rig#2a* and *Rig#2b*). [SDS] 0.3 wt%.

		THF 1 wt%		THF 4 wt%	
		Rig #2a	***Rig #2b***	***Rig #2a***	***Rig #2b***
CO_2 *enclathration rate:* $\frac{dn_{CO_2}}{dt} \times 10^4$ (mol/min)	Min	7.12	–	9.99	–
	Average	8.26	9.42	12.1	11.4
	Max	11.3	–	17.0	–
Total CO_2 *consumption in semi–continuous period:* $\Delta n_{CO_2}^{SV}\big\|_{tot}$ (mol)	Min	0.358	–	0.307	–
	Average	0.371	0.357	0.320	0.306
	Max	0.381	–	0.327	–

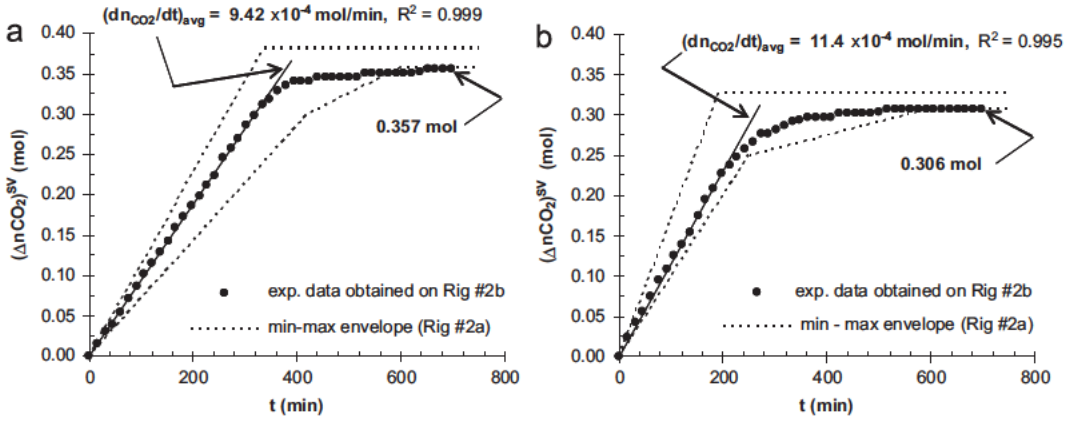


Fig. 10. Graphical comparison between the experimental data obtained in semi-continuous configuration with *Rig #2b* and the minimum and maximum values observed in the experiments conducted with *Rig #2a*. (a) [THF] 1 wt%; (b) [THF] 4 wt%; [SDS] 0.3 wt%.

experiments with *Rig #2a*. Experimental values of the CO_2 enclathration rates (minimum, average and maximum values) and total CO_2 consumptions during the semi continuous phase are summarized for the two rigs in the Table 2.

Fig. 10 and Table 2 show very clearly that the experiments carried out on two different experimental apparatus (of similar geometry) are consistent with each other.

The CO_2 enclathration rate is observed to increase slightly with THF concentration: the ratio $dn_{CO_2}/dt\big|_{avg}^{1\ wt\%(THF)}/dn_{CO_2}/dt\big|_{avg}^{4\ wt\%(THF)} \approx 0.68$ on (*Rig #2a*), and 0.83 on (*Rig #2b*). These results show that CO_2 enclathration in the CO_2 hydrate is accelerated when the quantity of THF used initially is 4 wt% instead of 1 wt%. This result cannot result from the thermodynamic effect of the THF since after the formation of the *first* hydrate, the THF is supposed to be totally consumed to form the mixed CO_2+THF hydrate (this assumption will be verified in the following). It is likely that a larger quantity of the mixed CO_2+THF hydrate initially dispersed in the bulk of the aqueous phase is advantageous for enhancing the CO_2 enclathration rate. As discussed previously in Section 4.1.3., it may be possible that the formation of this *first hydrate* preserves an open "porous" hydrate with a fine grained structure favourable to CO_2 diffusion and therefore to enclathration. However, this fundamental point is still not completely understood and deserves further additional experimental investigations.

Concerning the total CO_2 consumption in the semi continuous period, denoted $\Delta n_{CO_2}^{SV}\big|_{tot}$, this quantity slightly decreases with increasing THF concentration (see Table 2): the ratio $\Delta n_{CO_2}^{SV}\big|_{tot}^{1\ wt\%(THF)}/\Delta n_{CO_2}^{SV}\big|_{tot}^{4\ wt\%(THF)}$ is equal to 1.16 on (*Rig #2a*) and 1.17 on (*Rig#2b*). This result (ratio superior to unity) can be qualitatively understood as follows. For a larger initial amount of THF, a larger quantity of mixed CO_2+THF hydrates is formed, in which the proportion of water molecules relative to THF and CO_2 molecules is larger than that in CO_2 hydrates. This qualitative argument is substantiated below by a more detailed calculation.

The steady values reached by the reactor pressure and the CO_2 storage vessel pressure at the end of the experiments mean that CO_2 consumption and hydrate formation have ended. Assuming that: (i) there is no water left in the reactor for further hydrate formation, i.e., all water has been converted into hydrate; (ii) THF is fully converted into the mixed (sII) CO_2+THF hydrate which then remains stable and coexists with CO_2 hydrates (following our previous discussion and those of Shin et al. (2009)); and (iii) the quantity of THF and water present in the vapor phase is negligible (Ricaurte et al., 2012), it is possible to calculate the theoretical maximum quantity of CO_2 that can be enclathrated and compare it to our experimental estimate (and thus verify these above assumptions).

With a general notation, the CO_2 hydrate formula is $CO_2\ N_w^{(sI)}H_2O$, with $N_w^{(sI)}$ the number of water molecules per molecule of CO_2 (superscript (sI) refers to the structure of the CO_2 hydrate). Similarly, the mixed CO_2+THF hydrate formula is $N_{CO_2}^{(sII)}CO_2$ THF $N_w^{(sII)}H_2O$ with $N_w^{(sII)}$ the number of water molecules per molecule of THF and $N_{CO_2}^{(sII)}$ the number of CO_2 molecules per molecule of THF (superscript (sII) refers to the structure of mixed hydrate). Therefore, the theoretical expected molar quantity $n_{CO_2}^{H}\big|_{theo}$ of CO_2 trapped in the two hydrates (the CO_2 hydrate and the mixed hydrate) is expressed by Eq. (1):

$$n_{CO_2}^{H}\Big|_{theo} = \frac{n_{H_2O}|_i}{N_w^{(sI)}} \times \frac{N_w^{(sII)} \times n_{THF}|_i}{N_w^{(sI)}} + N_{CO_2}^{(sII)} \times n_{THF}|_i \qquad (1)$$

in which the initial molar quantities of water and THF are denoted by the subscript *i*.

We have fixed $N_w^{(sI)}$ to 7.3 for the CO_2 hydrate according to Uchida et al. (1995). In addition, Shin et al. (2009) demonstrated by experimental Raman measurements that the large cages of the CO_2+THF mixed hydrates would be dominantly occupied by THF molecules even if the hydrate is formed from off stoechimetric aqueous THF solutions, and their conclusions are in agreement with typical occupancies of large cavities which are greater than 95% (Sloan and Koh, 2008). Therefore, the value of $N_w^{(sII)} = 17$ has been adopted for the CO_2+THF mixed hydrate. As to $N_{CO_2}^{(sII)}$, Seo et al. (2003) have showed experimentally that the cages of (sII) mixed hydrates (CH_4+THF in this case) are not fully occupied by guests, and that the cage occupancy is dependent of the THF concentration. In addition, Martinez et al. (2008) found experi mentally, for mixed CO_2+THF hydrates, values of $N_{CO_2}^{(sII)}$ signifi cantly inferior to 2 and dependent on CO_2 pressure, consistent with the argument by Sloan and Koh (2008) that the occupancy of the small cavities varies widely depending on the guest composi tion, temperature and pressure (typical fractional occupancies of small cavities in simple hydrates from 0.3 to 0.9). However, in some cases, full occupancy of the (sII) hydrate structure may also be considered in a first approach as a practical simplifying assumption (Marinhas et al., 2007; Torré et al., 2011b). Accord ingly, two values of $N_{CO_2}^{(sII)}$ have been tested in the following calculations: $N_{CO_2}^{(sII)} = 1$ giving half occupancy by the CO_2 molecules of the $5^{12}6^4$ cages of (sII), and $N_{CO_2}^{(sII)} = 2$ for full occupancy.

From our experiments, the molar quantity of CO_2 trapped in the two hydrates $n_{CO_2}^{H}\big|_{exp}$ can be determined easily by a mass balance between the initial quantity of CO_2 after the solubiliza tion period and the final state (denoted by the subscript *f*) at the end of the semi continuous period. Thus, the total number of CO_2 contained into the hydrates is estimated by Eq. (2) as follows:

$$n_{CO_2}^{H}\Big|_{exp} = n_{CO_2}\big|_i + \Delta n_{CO_2}^{SV}\Big|_{tot} \quad n_{CO_2}^{g}\Big|_f \tag{2}$$

where:

$n_{CO_2}\big|_i = n_{CO_2}^{g}\big|_i + n_{CO_2}^{sol}\big|_i$ is the sum of the CO_2 present in the gas phase (denoted by superscript *g*) and the CO_2 solubilized (denoted by superscript *sol*) in the solution at initial conditions (T^R=293.1 K and P^R=2.70 MPa), $\Delta n_{CO_2}^{SV}\Big|_{tot}$ is the total CO_2 exiting the CO_2 storage vessel during the semi continuous period, and $n_{CO_2}^{g}\Big|_f$ is the remaining gas in the top of the reactor at the end of the semi continuous period (at T^R=275.15 K and P^R=1.89 MPa), taking into account the liquid volume expansion due to hydrate formation.

Form both the theoretical and the experimental point of views, it is possible to determine the ratio, denoted β, between the molar quantities of CO_2 trapped in the hydrates for [THF]=1 wt% and [THF]=4 wt% as:

$$\beta = \frac{n_{CO_2}^{H}\Big|^{[THF]\quad 1\ wt\%}}{n_{CO_2}^{H}\Big|^{[THF]\quad 4\ wt\%}} \tag{3}$$

Table 3 compares the results obtained from the model (Eq. (1)) and from the experiments (Eq. (2)) for the two THF concentra tions investigated. The solutions densities were calculated at 293.15 K using the density model developed previously in Ricaurte et al. (2012): 0.99768 g/cm^3 for [THF]=1 wt% and 0.99628 g/cm^3 for [THF]=4 wt%. The liquid to hydrate expansion factor (volume of hydrate/volume of liquid) has been considered equal to that of the (sI) CO_2 hydrate, i.e., 1.279 from Jung et al. (2010).

The theoretical and experimental values are in good agree ment, showing further evidence for the validity of the proposed mechanism and of the considered main assumptions (such as full conversion of water into hydrate, and full THF enclathration into the mixed (sII) CO_2+THF hydrate). In the conditions tested here, the results of the theoretical calculations are rather insensitive to the value of $N_{CO_2}^{(sII)}$ (as shown in Table 3 for values of $N_{CO_2}^{(sII)}$ equal to 1 and 2), because the quantity of the (sII) mixed CO_2+THF hydrate remains largely inferior to the quantity of the (sI) CO_2 hydrate. However, by matching the experimental quantities to the theoretical ones, it is possible to estimate the formula of the (sII) hydrate, assuming $N_w^{(sI)} = 7.30$ and $N_w^{(sII)} = 17$. The resolution of the equations (by an numerical optimization based on the least squared method) gives the better best result for $N_{CO_2}^{(sII)} \approx 1.3$. With this optimal number, the total quantity of CO_2 enclathrated in hydrates is equal to $n_{CO_2}^{H}\Big|_{theo}^{opt}$ =0.479 and 0.436 mol for [THF]=1 and 4 wt%, respectively (instead of 0.484 and 0.434 mol found experimentally), and β_{theo}^{opt}=1.099 (instead of 1.114 found experimentally).

Table 3
Comparison of the theoretical calculations to the experimental estimations.

	[THF] 1 wt%	[THF] 4 wt%
Theoretical values		
$n_{CO_2}^{H}\big\|_{theo}$ with $N_{CO_2}^{(sII)}$ 1	0.476	0.425
$\rightarrow \beta_{theo}$	1.121	
$n_{CO_2}^{H}\big\|_{theo}$ with $N_{CO_2}^{(sII)}$ 2	0.485	0.460
$\rightarrow \beta_{theo}$	1.053	
Experimental values		
$n_{CO_2}^{g}\big\|_i$(mol)	0.138	
$n_{CO_2}^{sol}\big\|_i$(mol)	0.0569	0.0583
$\Delta n_{CO_2}^{SV}\big\|_{tot}$ (mol)	0.371	0.320
$n_{CO_2}^{g}\big\|_f$(mol)	0.0819	
$n_{CO_2}^{H}\big\|_{exp}$(mol)	0.484	0.434
$\rightarrow \beta_{exp}$	1.114	

These results show very clearly how the addition of THF impacts negatively the total quantity of CO_2 enclathrated. The formation of the mixed hydrate, which is needed for promoting the formation of the (sI) CO_2 hydrate, *uses* a non negligible quantity of water (17 mol of water per mole of THF). This water is not available later for the formation of pure CO_2 hydrates and, accordingly, reduces the quantity of CO_2 enclathrated.

5. Concluding remarks and perspectives

To develop efficient hydrate based CO_2 separation processes, a research effort is still necessary to achieve high water to hydrate conversion, high selectivity of the hydrate phase towards CO_2 and sufficient enclathration rates (rapid kinetics), with the purpose to reach competitive costs with respect to realistic processes. One solution is to find appropriate additives to the aqueous phase. The combination of two water soluble additives a cyclic ether (THF) and a surfactant (SDS) has been investigated, focusing on their influence on hydrate equilibrium curves and CO_2 enclathration rate. At this stage, the gas used is pure CO_2: the selectivity of the hydrate phase toward CO_2 when the gas is a mixture of CO_2 and CH_4 will be investigated in a subsequent work.

Firstly, the equilibrium curves of the CO_2 hydrate and the mixed CO_2+THF hydrate (4 wt% THF in water) have been deter mined experimentally in the presence and absence of SDS (0.3 wt%). It is confirmed that, in presence of THF, the mixed CO_2+THF hydrate forms at higher temperatures and lower pressure in comparison to pure CO_2 hydrate equilibrium

conditions (THF is a strong thermodynamic promoter), and that SDS has no influence on the equilibrium curves of pure CO_2 hydrate and of the mixed CO_2+THF hydrate.

Secondly, kinetic studies carried out in quiescent hydrate forming conditions both in batch and in semi continuous reactor configurations reveal that the two additives must be used in combination to achieve high conversion into hydrates and rapid CO_2 enclathration rates, at least for a temperature decrease down to 275 K and initial CO_2 pressure in the range of 3 MPa. Experiments in a batch reactor configuration allow defining first the "optimum" operating pressure conditions for the ensuing semi continuous isobaric experiments, in which the conversion of all the water present into CO_2 hydrates is achieved in a reasonable amount of time and in quiescent conditions. The measured CO_2 enclathration rate in the latter semi continuous (isobaric) conditions increases only slightly with THF concentration in water. From 1 to 4 wt%, the quantity of CO_2 enclathrated is somewhat lower when THF concentration is higher, due to the formation of a mixed THF+CO_2 hydrate which contains a non negligible quantity of water. Finally, the proposed mechanism, in which the mixed CO_2+THF hydrate phase forms firstly in the bulk of the aqueous phase and promotes (through the presence of a few crystallites) the ensuing formation of CO_2 hydrate, agrees with all of our observations, measurements and calculations, and is consistent with the already published data for mixed hydrates containing THF, particularly those by Seo et al. (2003) and by Shin et al. (2009). Nevertheless, additional investigations are necessary to understand the reason why this combination of additives (THF+SDS) is so efficient, and what is the exact role played by the surfactant.

Other experiments are actually in progress in our laboratory with this couple of additives to: (i) quantify the selectivity of the CO_2 separation when the gas is a mixture of CO_2 and CH_4 (Ricaurte et al., 2011), (ii) characterize the transient hydrate structures using Raman spectroscopy, and (iii) determine precisely the absolute cage occupancy of the guests (THF and CO_2) in the (sII) structure. More generally, the additive combination of a kinetic hydrate promoter with a thermodynamic hydrate promoter is potentially very promising for improving hydrate based CO_2 capture processes.

Acknowledgments

The authors would like to owe great thanks to the technical staff of the University of Pau: J. Diaz and L. Marlin are particularly acknowledged for their good technical work and assistance on the experimental rigs. CCL (Communauté des Communes de Lacq), CG64 (Conseil Général des Pyrénées Atlantiques), ANR (Agence Nationale de la Recherche) through SECOHYA project, Total E&P ("Gas Solutions" R&D Project) and Fundayacucho from Venezuela are gratefully acknowledged for partial financial support of this work.

Appendix A. Statistical analysis concerning the data of reactor pressure at inflexion points

All the data considered for this statistical analysis (total of 33 inflexion points) has been computed using the software Statgraphics®. The result of the analysis is simply illustrated using a Box and Whiskers diagram shown in Fig. 11. No outlier and no suspect point were identified. The average value was estimated to be $P^R_{avg} = 1.89 \pm 0.08$ MPa.

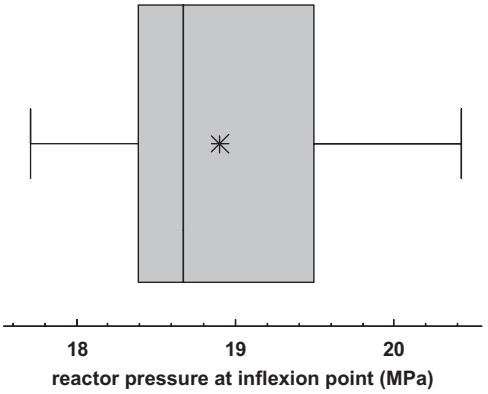


Fig. 11. Box and whiskers diagram of the inflexion point pressure data. Number of values 33; Min value (left whisker) 1.77 MPa; Max value (right whisker) 2.04 MPa; the mean value (symbol in the middle of the box) 1.89 MPa; the median (vertical line in the box) 1.87 MPa; standard deviation 0.08 MPa.

References

Bakshi, M.S., 1993. Micelle formation by anionic and cationic surfactants in binary aqueous solvents. J. Chem. Soc. Fraraday Trans 89 (24), 4323–4326.
Delahaye, A., Fournaison, L., Marinhas, S., Chatti, I., Petitet, J.-P., Dalmazzone, D., Fürst, W., 2006. Effect of THF on equilibrium pressure and dissociation enthalpy of CO_2 hydrates applied to secondary refrigeration. Ind. Eng. Chem. Res. 45, 391–397.
Di Profio, P., Arca, S., Germani, R., Savelli, G., 2005. Surfactant promoting effects on clathrate hydrate formation: Are micelles really involved? Chem. Eng. Sci. 60, 4141–4145.
Duc, N.H., Chauvy, F., Herri, J.-M., 2007. CO_2 capture by hydrate crystallization – A potential solution for gas emission of steelmaking industry. Energ. Conv. Manage. 48, 1313–1322.
Eslamimanesh, A., Mohammadi, A.H., Richon, D., Naidoo, P., Ramjugernath, D., 2012. Application of gas hydrate formation in separation processes: A review of experimental studies. J. Chem. Thermodyn. 46, 62–71.
Figueroa, J.D., Fout, T., Plasynski, S., McIlvried, H., Srivastava, R.D., 2008. Advances in CO2 capture technology—The U.S. Department of Energy's Carbon Sequestration Program. Int. J. Greenh. Gas Control 2 (1), 9–20.
Gayet, P., Dicharry, C., Marion, G., Graciaa, A., Lachaise, J., Nesterov, A., 2005. Experimental determination of methane hydrate dissociation curve up to 55 MPa by using a small amount of surfactant as hydrate promoter. Chem. Eng. Sci. 60, 5751–5758.
Jung, J.W., Espinoza, D.N., Santamarina, J.C., 2010. Properties and phenomena relevant to CH_4-CO_2 replacement in hydrate-bearing sediments. J. Geophys. Res. 115 (B10102), 1–16.
Kang, S.-P., Lee, J.-W., 2010. Kinetic behaviors of CO_2 hydrates in porous media and effect of kinetic promoter on the formation kinetics. Chem. Eng. Sci. 65, 1840–1845.
Koh, C.A., Sloan, E.D., Sum, A.K., Wu, D.T., 2011. Fundamental and applications of gas hydrates. Annu. Rev. Chem. Biomol. Eng. 2, 237–257.
Kuramochi, T., Ramírez, A., Turkenburg, W., Faaij, A., 2011. Techno-economic assessment and comparison of CO_2 capture technologies for industrial processes: preliminary results for the iron and steel sector. Energy Procedia 4, 1981–1988.
Linga, P., Kumar, R., Lee, J.D., Ripmeester, J., Englezos, P., 2010. A new apparatus to enhance the rate of gas hydrate formation: Application to capture of carbon dioxide. Int. J. Greenh. Gas Control 4, 630–637.
Liu, N., Gong, G., Liu, D., Xie, Y., 2008a. Effect of additives on carbon dioxide hydrate formation. In: Proceedings of the 6th International Conference on Gas Hydrates (ICGH 2008), Vancouver, Canada, July 6–10, 2008.
Liu, N., Zhang, G.-C., Rogers, R.E., 2008b. Effect of additives on the formation of carbon dioxide hydrate. Natural Gas Ind. 28 (12), 104–106.
Lo, C., Zhang, J., Somasundaran, P., Lee, J.W., 2010. Raman spectroscopic studies of surfactant effect on the water structure around hydrate guest molecules. J. Phys. Chem. Lett. 1, 2676–2679.
Lopez-Grio, S., Baeza-Baeza, J.J., Garcia-Alvarez-Coque, M.C., 1998. Influence of the addition of modifiers on solote-micelle interaction in Irbid micellar liquid chromatography. Chromatography 48 (9–10), 655–663.
Makino, T., Sugahara, T., Ohgaki, K., 2005. Stability Boundaries of Tetrahydrofuran+Water System. Journal of Chemical. Eng. Data 50, 2058–2060.
Marinhas, S., Delahaye, A., Fournaison, L., 2007. Solid fraction modelling for CO_2 and CO_2+THF hydrate slurries used as secondary refrigerants. Int. J. Refrig. 30, 758–766.
Martinez, M.C., Dalmazzone, D., Fürst, W., Delahaye, A., Fournaison, L., 2008. Thermodynamic properties of THF+CO_2 hydrates in relation with refrigeration applications. AiChE J. 54 (4), 1088–1095.

Moudrakovski, I.L., Ratcliffe, C.I., Ripmeester, J.A., 2001. Probing Transient Hydrate Structures with Hyperpolarized ^{129}Xe NMR Spectroscopy: A Metastable Structure II Hydrate of Xe. Angew. Chem. Int. Ed. 40 (20), 3890–3892.

Okutani, K., Kuwabara, Y., Mori, Y.H., 2008. Surfactant effects on hydrate formation in an unstirred gas/liquid system: An experimental study using methane and sodium alkyl sulfates. Chem. Eng. Sci. 63, 183–194.

Rana, D., Neale, G.H., Hornof, V., 2002. Surface tension of mixed surfactant systems: lignosulfonate and sodium dodecyl sulfate. Colloid Polym. Sci. 280, 775–778.

Ribeiro Jr., C.P., Lage, P.L.C., 2008. Modelling of hydrate formation kinetics: State-of-the-art and future directions. Chem. Eng. Sci. 63, 2007–2034.

Ricaurte,* M., Torré, J.-P., Broseta, D., Diaz, J., Dicharry, C., Renaud, X., 2011. CO_2 removal from a CO_2-CH_4 gas mixture by hydrate formation: evaluation of additives and operating conditions. In: Proceedings of the 7th International Conference on Gas Hydrates (ICGH 2011), Edinburgh, Scotland, United Kingdom, July 17–21, 2011.

Ricaurte, M., Torré, J.-P., Asbai, A., Broseta, D., Dicharry, C., 2012. Experimental data, modeling, and correlation of carbon dioxide solubility in aqueous solutions containing low concentrations of clathrate hydrate promoters: application to CO_2–CH_4 gas mixtures. Ind. Eng. Chem. Res. 51 (7), 3157–3169.

Rogers, R., Zhang, G., Dearman, J., Woods, C., 2007. Investigations into surfactant/gas hydrate relationship. J. Pet. Sci. Eng. 56, 82–88.

Rovetto, L.J., Bowler, K.E., Stadterman, L.L., Dec, S.F., Koh, C.A., Sloan Jr., E.D., 2007. Dissociation studies of CH_4–C_2H_6 and CH_4–CO_2 binary gas hydrates. Fluid Phase Equilibria 261, 407–413.

Sabil, K.M., Duarte, A.R.C., Zevenbergen, J., Ahmad, M.M., Yusup, S., Omar, A.A., Peters, C.J., 2010. Kinetic of formation for single carbon dioxide and mixed carbon dioxide and tetrahydrofuran hydrates in water and sodium chloride aqueous solution. Int. J. Greenh. Gas Control 4, 798–805.

Sabil, K.M., Witkamp, G.-J., Peters, C.J., 2009. Phase equilibria of mixed carbon dioxide and tetrahydrofuran hydrates in sodium chloride aqueous solutions. Fluid Phase Equilibria 284, 38–43.

Seo, Y.-T., Lee, H., Moudrakovski, I., Ripmeester, J.A., 2003. Phase behavior and structural characterization of coexisting pure and mixed clathrate hydrates. ChemPhysChem 4, 379–382.

Schicks, J.M., Naumann, R., Erzinger, J., Hester, K.C., Koh, C.A., Sloan, E.D., 2006. Phase transitions in mixed gas hydrates: experimental observations versus calculated data. J. Phys. Chem. B 110 (23), 11468–11474.

Schicks, J.M., Ripmeester, J.A., 2004. The coexistence of two different methane hydrate phases under moderate pressure and temperature conditions: kinetic versus thermodynamic products. Angew. Chem. Int. Ed. 43 (25), 3310–3313.

Shin, H.J., Lee, Y.-J., Im, Y.-H., Han, K.W., Lee, J.-W., Lee, Y., Lee, J.D., Jang, W.-Y., Yoon, J.-H., 2009. Thermodynamic stability, spectroscopic identification and cage occupation of binary CO_2 clathrate hydrates. Chem. Eng. Sci. 64 (24), 5125–5130.

Sloan, E.D., 2003. Fundamental principles and applications of natural gas hydrates. Nature 426 (20), 353–359.

Sloan, E.D., Koh, C.A., 2008. Clathrate hydrates of natural gases, 3rd edition CRC Press, New York.

Staykova, D.K., Kuhs, W.F., Salamatin, A.N., Hansen, T., 2003. Formation of porous gas hydrates from ice powders:diffraction experiments and multistage model. J. Phys. Chem. B 107 (37), 10299–10311.

Sum, A.K., Burruss, R.C., Sloan, E.D., 1997. Measurement of clathrate hydrates via raman spectroscopy. J. Phys. Chem. B 101 (38), 7371–7377.

Sum, A.K., Koh, C.A., Sloan, E.D., 2009. Clathrate hydrates: from laboratory science to engineering practice. Ind. Eng. Chem. Res. 48, 7457–7465.

Sun, C., Li, W., Yang, X., Li, F., Yuan, Q., Mu, L., Chen, J., Liu, B., Chen, G., 2011. Progress in research of gas hydrate. Chinese J. Chem. Eng. 19 (1), 151–162.

Torré, J.-P., Dicharry, C., Ricaurte, M., Daniel-David, D., Broseta, D., 2011a. CO_2 capture by hydrate formation in quiescent conditions: in search of efficient kinetic additives. Energy Procedia J. 4(C), 621–628.

Torré, J.-P., Dicharry, C., Ricaurte, M., Broseta, D., Diaz, J., Renaud, X., 2011b. CO_2 enclathration in a semi-continuous quiescent hydrate-forming reactor operated with pure CO_2 and water soluble additives. In: Proceedings of the 7th International Conference on Gas Hydrates (ICGH 2011), Edinburgh, 2011.

Uchida, T., Hondoh, T., Mae, S., Kawabata, J., 1995. Physical data of CO_2 hydrate. Direct Ocean Disposal of Carbon Dioxide. Terra Scientific Publishing Company 45–61.

Uchida, T., Moriwaki, M., Takeya, S., Ikeda, I.Y., Ohmura, R., Nagao, J., Minagawa, H., Ebinuma, T., Narita, H., Gohara, K., Mae, S., 2004. Two-step formation of methane–propane mixed gas hydrates in a batch-type reactor. AIChE J. 50 (2), 518–523.

Vlahakis, J.G., Chen, H.-S., Suwandi, M.S., Barduhn, A.J., 1972. The growth rate of ice crystals: properties of carbon dioxide hydrates, a review of properties of 51 gas hydrates. Research and Development Progress Report 830, Office of Saline Water, United States Department of the Interior.

Watanabe, K., Imai, S., Mori, Y.H., 2005. Surfactant effects on hydrate formation in an unstirred gas/liquid system: An experimental study using HFC-32 and sodium dodecyl sulphate. Chem. Eng. Sci. 60, 4846–4857.

Yoslim, J., Linga, P., Englezos, P., 2010. Enhanced growth of methane–propane clathrate hydrate crystals with sodium dodecyl sulfate, sodium tetradecyl sulfate, and sodium hexadecyl sulfate surfactants. J. Cryst. Growth 313 (1), 68–80.

Zhang, J.S., Lee, S., Lee, J.W., 2007. Solubility of sodium dodecyl sulfate near propane and carbon dioxide hydrate-forming conditions. J. Chem. Eng. Data 52, 2480–2483.

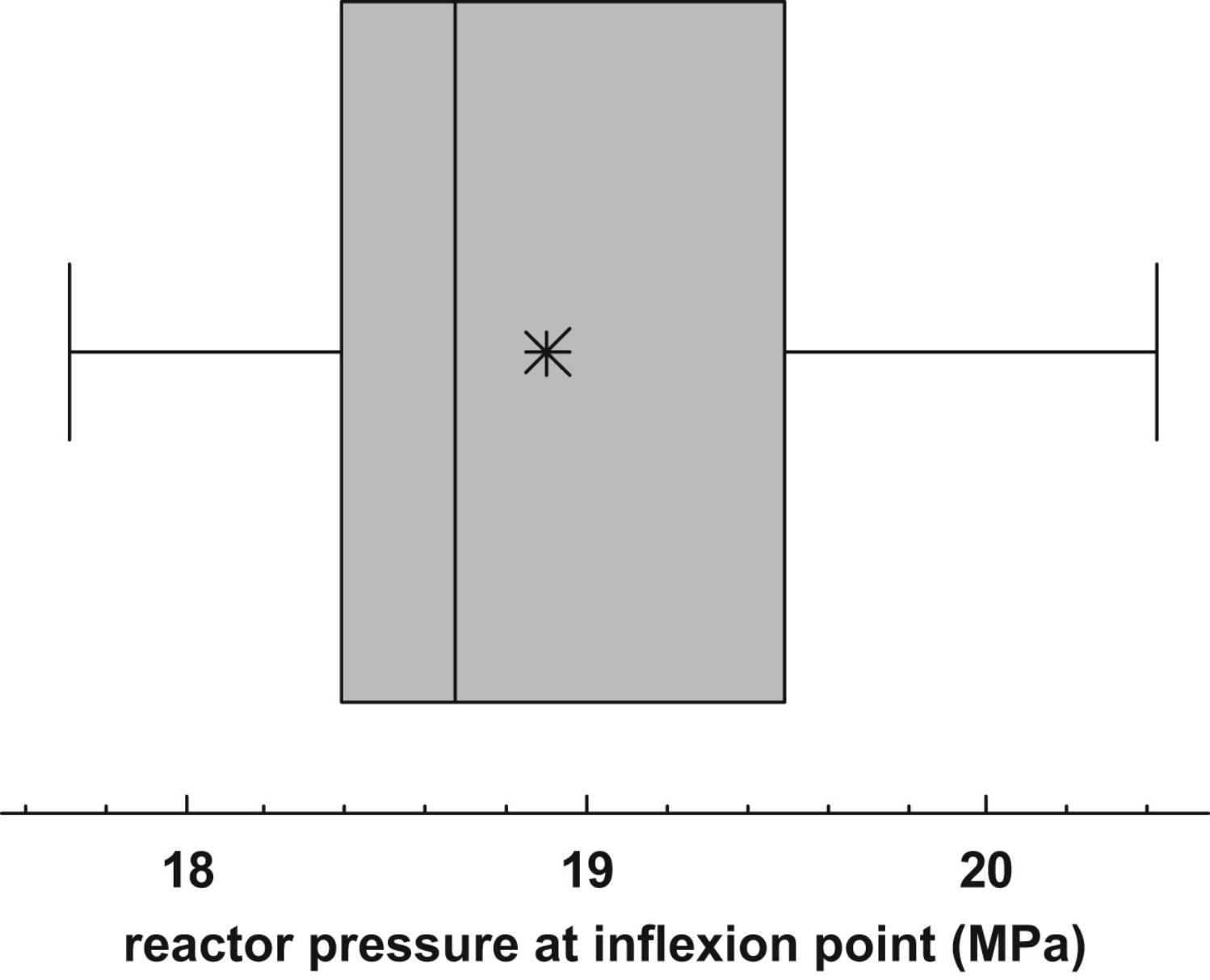
Zhang, J., Lee, J.W., 2009. Enhanced kinetics of CO_2 hydrate formation under static conditions. Ind. Eng. Chem. Res. 48, 5934–5942.

Zhang, J.S., Lo, C., Somasundaran, P., Lee, J.W., 2010. Competitive adsorption between SDS and carbonate on tetrahydrofuran hydrates. J. Colloid Interface Sci. 341, 286–288.

Zhang, J.S., Lo, C., Somasundaran, P., Lu, S., Couzis, A., Lee, J.W., 2008. Adsorption of sodium dodecyl sulfate at thf hydrate/liquid interface. J. Phys. Chem. C 112 (32), 12381–12385.

Zhong, Y., Rogers, R.E., 2000. Surfactant effects on gas hydrate formation. Chem. Eng. Sci. 55, 4175–4187.

Zhu, C., Li, Y., Wang, W., Chen, Y., Chen, P., Liu, H., Liang, B., 2011. Effect of surfactants on the hydrate formation kinetics of carbon dioxide. In: Proceedings of the 7th International Conference on Gas Hydrates (ICGH 2011), Edinburgh, Scotland, United Kingdom, July 17–21, 2011.


18
19
20
reactor pressure at inflexion point (MPa)